

# Rothamsted Repository Download

## A - Papers appearing in refereed journals

Trocza, B. J., Richardson, E., Homem, R. A. and Davies, T. G. E. 2018. An analysis of variability in genome organisation of intracellular calcium release channels across insect orders. *Gene*. 670 (5 September), pp. 70-86.

The publisher's version can be accessed at:

- <https://dx.doi.org/10.1016/j.gene.2018.05.075>

The output can be accessed at: <https://repository.rothamsted.ac.uk/item/847vv/an-analysis-of-variability-in-genome-organisation-of-intracellular-calcium-release-channels-across-insect-orders>.

© 21 May 2018, CC-BY terms apply



## Research paper

# An analysis of variability in genome organisation of intracellular calcium release channels across insect orders



Bartłomiej J. Troczka, Ewan Richardson, Rafael A. Homem, T.G. Emyr Davies\*

Biointeractions and Crop Protection Department, Rothamsted Research, Harpenden AL5 2JQ, UK

## ARTICLE INFO

## Keywords:

Ryanodine receptor  
Inositol 1,4,5-trisphosphate receptor  
Insect

## ABSTRACT

Using publicly available genomic data, combined with RT-PCR validation, we explore structural genomic variation for two major ion channels across insect classes. We have manually curated ryanodine receptor (RyR) and inositol 1,4,5-trisphosphate receptor (IP<sub>3</sub>R) ORFs and their corresponding genomic structures from 26 different insects covering major insect orders. We found that, despite high protein identity for both RyRs (> 75%) and IP<sub>3</sub>Rs (~67%), the overall complexity of the gene structure varies greatly between different insect orders with the simplest genes (fewest introns) found in Diptera and the most complex in Lepidoptera. Analysis of intron conservation patterns indicated that the majority of conserved introns are found close to the 5' end of the channels and in RyR around the highly conserved mutually exclusive splice site. Of the two channels the IP<sub>3</sub>Rs appear to have a less well conserved organisation with a greater overall number of unique introns seen between insect orders. We experimentally validated two of the manually curated ORFs for IP<sub>3</sub>Rs and confirmed an atypical (3799aa) IP<sub>3</sub>R receptor in *Myzus persicae*, which is approximately 1000 amino acids larger than previously reported for IP<sub>3</sub>Rs.

## 1. Introduction

Recent advances in sequencing technologies have led to a rapid increase in the number of publicly available genomes, including those of insects. The insect genomes have been found to be incredibly diverse in size; the smallest genome, that of *Belgica antarctica*, comprising only 99 megabases (Kelley et al., 2014) whilst the ~6.5 gigabase genome of *Locusta migratoria* is the largest genome within the animal kingdom (Wang et al., 2014). This diversity in genome size is also reflected in gene architecture complexity; in other words, despite a high degree of similarity at the protein level, the genomic architecture of genes can vary greatly between insect orders. Recent genome annotation efforts suggest that insect ryanodine receptors (RyRs) are a classic example of this type of complexity e.g. the number of exons present within this gene can vary from 26 in the fruit fly *D. melanogaster* (Takeshima et al., 1994) to 55 in the red flour beetle *T. castaneum* (Liu et al., 2014) and 98 in aphids (e.g. *Myzus persicae* and *Acyrtosiphon pisum*) (Troczka et al., 2015a; Dale et al., 2010).

Ryanodine receptors (RyRs) and inositol 1,4,5-trisphosphate receptors (IP<sub>3</sub>Rs) are large and complex calcium release channels; whilst RyRs are primarily located in the endo (sarco) plasmic reticulum of

muscle cells, IP<sub>3</sub>Rs and RyRs are also found in many other cell types (Foskett et al., 2007; Hamilton and Serysheva, 2009). Both types of channels are inherently involved in the release of Ca<sup>2+</sup> from internal stores - however, each channel has a distinct biological function; RyRs are involved in the regulation of calcium release during excitation-contraction coupling in muscle tissues and are primarily activated either by free Ca<sup>2+</sup> or direct interaction with Ca<sub>v</sub>1.2 located in the plasma membrane (depending on channel isoform) (Fill and Copello, 2002), whereas IP<sub>3</sub>Rs are involved in complex spatio-temporal Ca<sup>2+</sup> dynamics that have been implicated in a wide variety of biological functions from gene expression and apoptosis to learning and memory, and are primarily activated by the secondary messenger inositol 1,4,5-trisphosphate (IP<sub>3</sub>) (Foskett et al., 2007).

Partly due to the effectiveness and consequent commercial success of diamide insecticides, namely flubendiamide and chlorantraniliprole, which act as selective activators of insect RyRs (Cordova et al., 2006; Ebginghaus-Kintscher et al., 2007), these channels have recently been receiving a considerable amount of attention from the scientific community, especially from researchers interested in understanding the mechanisms underlying the development of diamide resistance. Consequently, the number of RyR cDNAs being sequenced and cloned from

**Abbreviations:** ORF, open reading frame; RyR, ryanodine receptor; IP<sub>3</sub>R, inositol 1,4,5-trisphosphate receptor; RT-PCR, reverse transcription polymerase chain reaction; TM, transmembrane

\* Corresponding author.

E-mail addresses: [bartek.troczka@rothamsted.ac.uk](mailto:bartek.troczka@rothamsted.ac.uk) (B.J. Troczka), [ewan.richardson@rothamsted.ac.uk](mailto:ewan.richardson@rothamsted.ac.uk) (E. Richardson), [rafael.homem@rothamsted.ac.uk](mailto:rafael.homem@rothamsted.ac.uk) (R.A. Homem), [emyr.davies@rothamsted.ac.uk](mailto:emyr.davies@rothamsted.ac.uk) (T.G.E. Davies).

<https://doi.org/10.1016/j.gene.2018.05.075>

Received 30 January 2018; Received in revised form 15 May 2018; Accepted 18 May 2018

Available online 21 May 2018

0378-1119/ © 2018 The Authors. Published by Elsevier B.V. This is an open access article under the CC BY license (<http://creativecommons.org/licenses/by/4.0/>).

**Table 1**  
Summary of annotated sequences for ryanodine receptors.

Order	Species	Exon	Accession no.	Protein (AA)	Gene (bp)	Genome (Mb)
Diptera	<i>Anopheles gambiae</i> (African malaria mosquito)	29	XP_318561	5109	29,159	265.027
	<i>Ceratitis capitata</i> (Mediterranean fruit fly)	31	XP_012158404	5140	38,927	479.048
	<i>Drosophila melanogaster</i> (fruit fly)	26	NP_001246211	5134	24,856	143.726
	<i>Musca domestica</i> (house fly)	30	XP_011296550	5127	71,276 <sup>a</sup>	750.404
	<i>Belgica antarctica</i> (Antartic midge)	28		5088	21,215	89.5837
Hymenoptera	<i>Apis mellifera</i> (honey bee)	54		5107	30,266	250.287
	<i>Bombus terrestris</i> (buff-tailed bumblebee)	54	XP_012175586	5108	37,861	248.654
	<i>Nasonia vitripennis</i> (jewel wasp)	56	XP_003425568	5099	30,168	295.781
	<i>Megachile rotundata</i> (alfalfa leafcutting bee)	55		5109	30,560	272.661
	<i>Harpegnathos saltator</i> (Jerdon's jumping ant)	54		5101	41,561	294.466
Coleoptera	<i>Tribolium castaneum</i> (red flour beetle)	54	NP_001308588	5094	97,420	165.944
	<i>Dendroctonus ponderosae</i> (mountain pine beetle)	70		5137	50,615	252.848
	<i>Anoplophora glabripennis</i> (Asian longhorned beetle)	63		5091	30,477	707.712
	<i>Hypothenemus hampei</i> (coffee berry borer)	66		5107	21,874	151.272
Hemiptera	<i>Myzus persicae</i> (green peach aphid)	98	AJA41114	5101	59,601	347.313
	<i>Cimex lectularius</i> (bed bug)	91	XP_014249567	5093	62,674	650.478
	<i>Rhodnius prolixus</i> (Assassin bug)	103		5103	117,911	706.824
	<i>Ferrisia virgata</i> (striped mealybug)	100		4982	47,978	304.571
Lepidoptera	<i>Bombyx mori</i> (domestic silkworm)	110		5121	137,409	481.819
	<i>Papilio xuthus</i> (Asian swallowtail butterfly)	109		5124	92,730	243.89
	<i>Manduca sexta</i> (tobacco hornworm)	110		5127	114,469	419.424
	<i>Phoebis sennae</i> <sup>a</sup> (cloudless sulphur butterfly)	108 <sup>a</sup>		5109	97,628	287.49
	<i>Spodoptera frugiperda</i> (fall armyworm)	109		5127	131,979	358.048
Acari	<i>Tetranychus urticae</i> (two-spotted spider mite)	12	XP_015783312	5200	18,117	90.8286
Other orders	<i>Blattella germanica</i> (German cockroach)	103		5120	159,200	2037.2
	<i>Pediculus humanus corporis</i> (human body louse)	78	XP_002424547	5058	23,243	110.781
	<i>Locusta migratoria</i> <sup>b</sup> (migratory locust)	103 <sup>b</sup>		5130	371,221	5759.8

<sup>a</sup> The ORF in *Pheobes sennae*, although located on a single scaffold, remains incomplete as exons 48, 102, 103 and part of exon 54 are missing. This is likely due to gaps in the published scaffold sequence.

<sup>b</sup> The ORF in *Locusta migratoria* also remains incomplete with predicted exons 44, 68 and 78 being missing and sequencing gaps are present in exons 52, 58, 80 and 88. Due to missing sequence information the number of predicted exons for these two genes differs on manual curation compared with the webscipio/gene painter analysis.

a variety of agriculturally important pest species has rapidly increased (Nauen and Steinbach, 2016; Troczka et al., 2017). In comparison, IP<sub>3</sub>Rs remain significantly understudied in invertebrates. To date, only two insect IP<sub>3</sub>Rs have been cloned and experimentally tested; one from the *Drosophila melanogaster* (Yoshikawa et al., 1992) and the other from *Tribolium castaneum* (Liu et al., 2014). Functional expression of the *D. melanogaster* IP<sub>3</sub>R showed that its physiological properties are highly conserved in relation to its mammalian counterparts (Srikanth et al., 2004). The genomic organisation of IP<sub>3</sub>Rs however remains largely uncharacterised in insects - to date only *T. castaneum* IP<sub>3</sub>R has had its intron/exon organisation reported (Liu et al., 2014).

Although automated gene prediction tools are indispensable for genome annotations, these can occasionally generate incorrect gene structures (Yandell and Ence, 2012). The aim of this paper has therefore been to catalogue and validate a number of RyR and IP<sub>3</sub>R protein sequences, together with their genomic organisations, in 26 representative insect species, to help with future annotation of calcium release channels in genomic datasets and to further our understanding of the receptors' diversity in insects. Understanding the genomic structures of the insect channels could also contribute to a deeper appreciation of the evolution and regulation of these genes. IP<sub>3</sub>Rs are also candidate targets for the development of new classes of anti-insect molecules.

## 2. Materials and methods

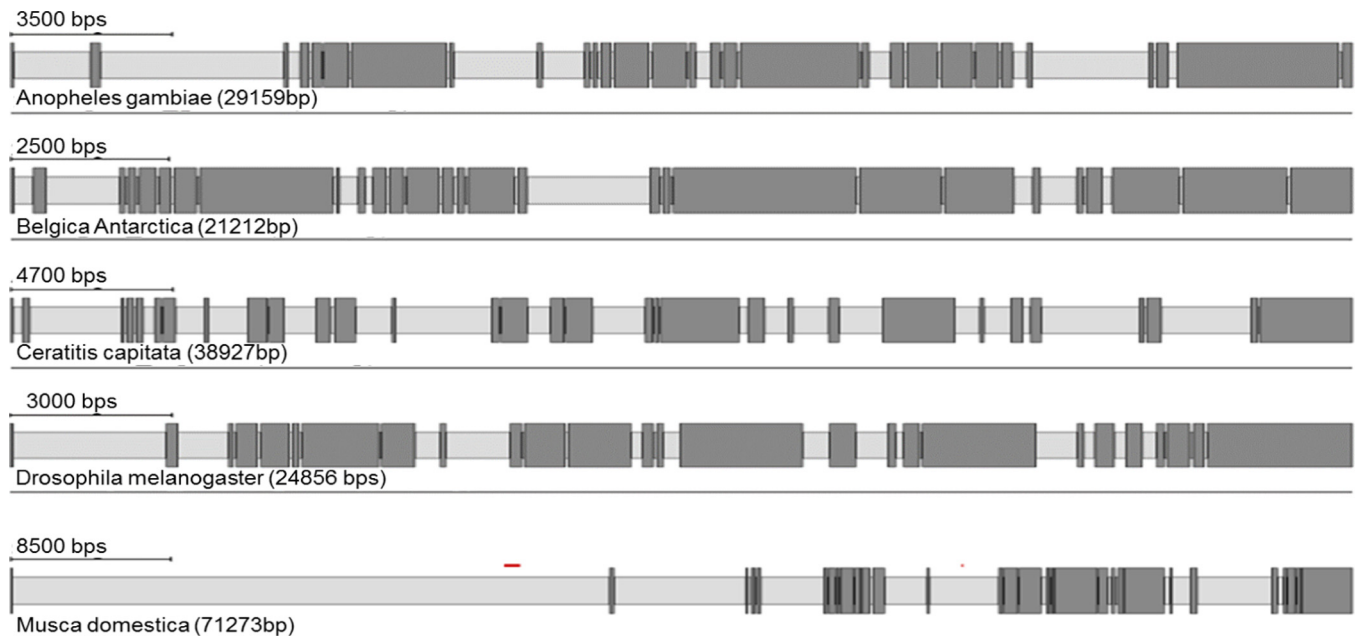
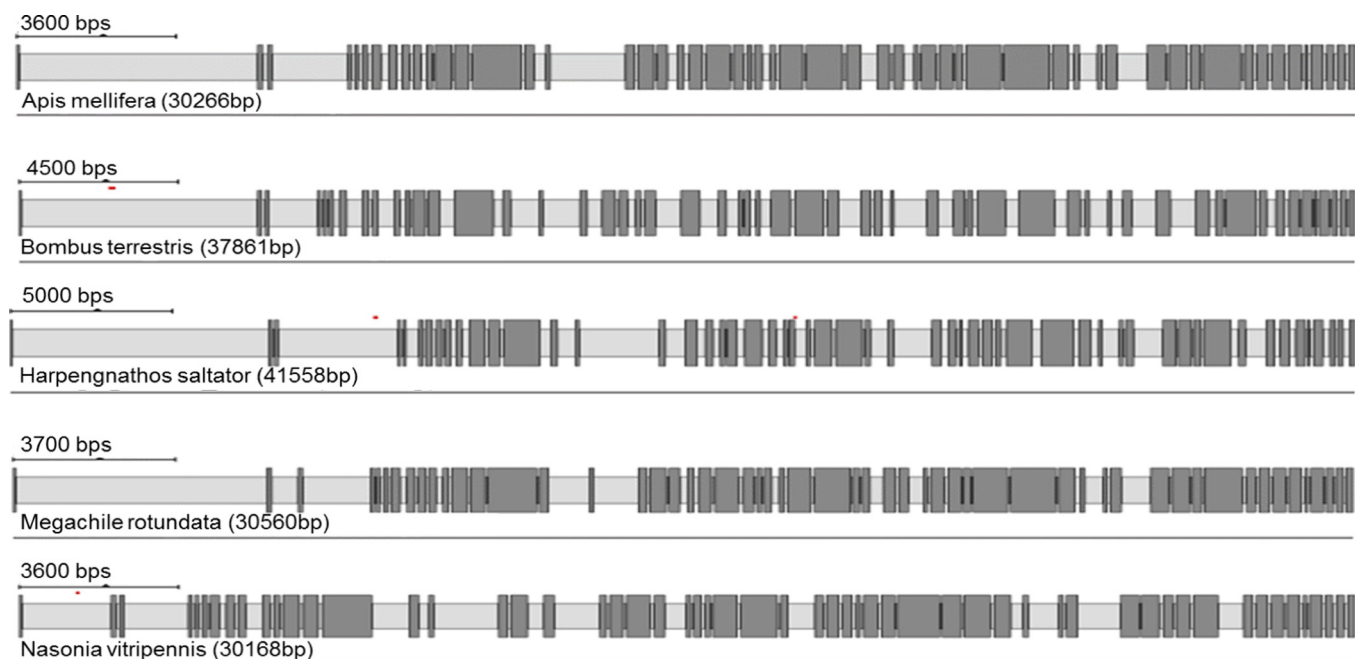
### 2.1. In silico annotation and data mining

26 insect species from 5 insect orders with publicly available genomes (Diptera, Coleoptera, Hemiptera, Hymenoptera, Lepidoptera), 3 representatives of other insect orders (Blattellidae, Locusta, Phthiraptera) and one outlying acarine species (*Tetranychus urticae*) of the order Trombidiformes were included in the study (for a list of

genome projects used for data generation see Appendix A). For each of the 5 main insect orders studied, a 'reference species' sequence was chosen to BLAST against the other available genomes within that particular order. The choice of 'reference species' sequence was based on a previous cloning and annotation of the sequence and the overall quality of the available genome. In the case of RyR the 5 reference species were: Dipteran = *D. melanogaster*, Hemipteran = *Myzus persicae*, Coleopteran = *T. castaneum*, Hymenopteran = *Apis mellifera*, Lepidopteran = *Bombyx mori*. For the IP<sub>3</sub>R, *D. melanogaster* and *T. castaneum* IP<sub>3</sub>Rs were the only sequences available to be used as a reference. PCR validation of Hymenopteran and Hemipteran IP<sub>3</sub>R genes was carried out to confirm the automated annotations. Three additional species, *Blattella germanica*, *Locusta migratoria* and *Pediculus humanus corporis*, were chosen for analysis based on the 'completeness' of their RyR genomic region, low contig fragmentation and few intra-contig gaps, determined by tblastn results against the WGS contig database with a reference RyR sequence.

Relevant contigs were downloaded from the NCBI database and manually curated using Geneious software v. 8.1.3 (Biomatters, Ltd., New Zealand). Translated exon sequences from the 'reference species' were blasted against databases created in Geneious using the tblastn algorithm. Megablast was used when DNA sequences were compared. Multiple sequence alignments were done using the MAFFT plugin in Geneious.

Splign (<https://www.ncbi.nlm.nih.gov/sutils/splign/splign.cgi>) (Kapustin et al., 2008) and manual curation was used to map intron-exon junctions, using as a curation guide the sequences of the most closely related reference species. Predicted RyR ORFs were extracted from the genomic sequence and validated with multiple alignments against a database of 25 manually curated insect and mammalian RyR sequences obtained from the NCBI database (see Appendix B). Gene structure graphs were generated using WebScipio (<http://www.webscipio.org/>) (Hatje et al., 2011). A web version of GenePainter

**Diptera****Hymenoptera**

**Fig. 1.** RyR gene structures generated by Webscipio. Dark grey regions correspond to exons. Red dashes indicate gaps in the sequencing, blue dashes indicate some uncertainty in intron assignment (non-canonical intron boundaries). (For interpretation of the references to colour in this figure legend, the reader is referred to the web version of this article.)

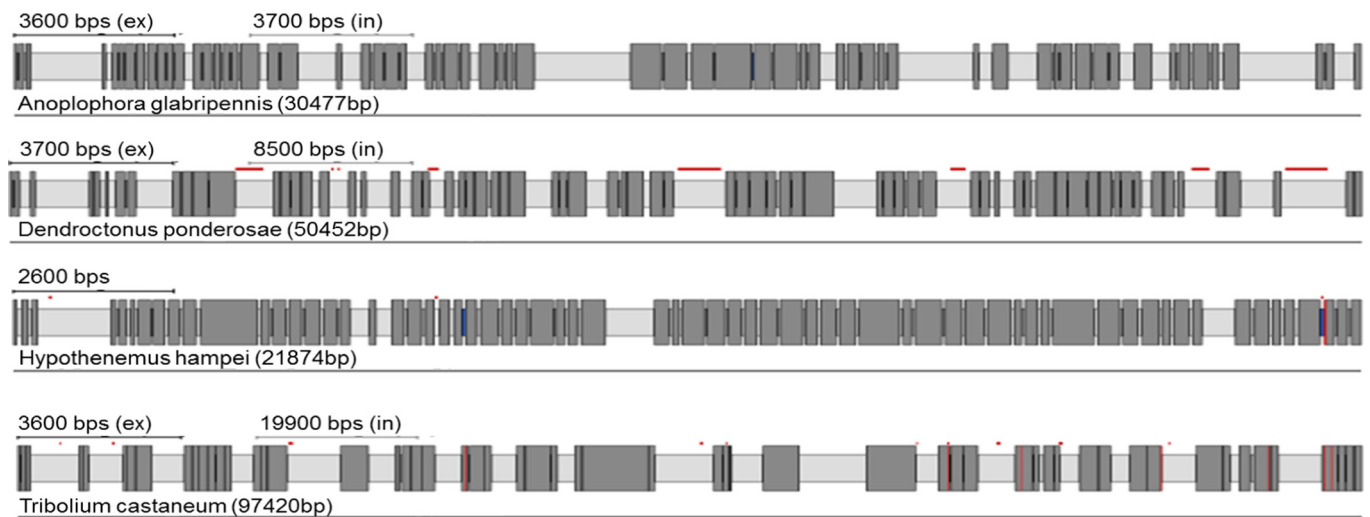
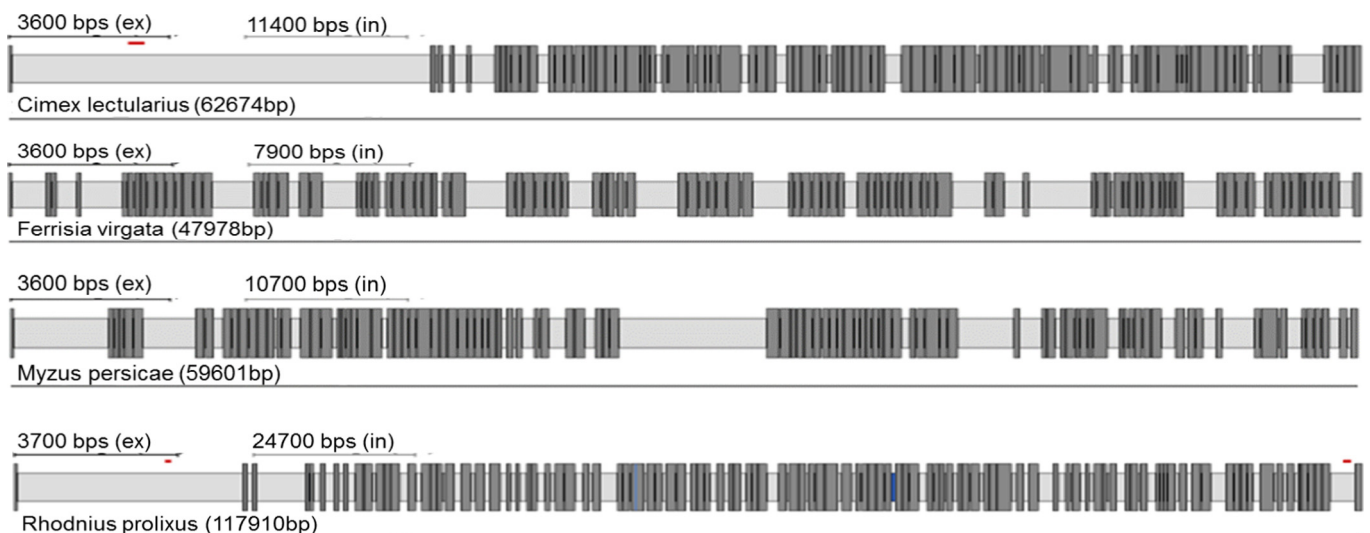
(<http://www.motorprotein.de/genepainter/genepainter>) (Muhlhausen et al., 2015; Hammesfahr et al., 2013) was then used to generate intron phylogeny analysis based on the structure of the genes.

Structural features of analysed RyRs were determined based on multiple alignments of protein sequences with the previously annotated *P. xylostella* RyR (NCBI accession AET09964) (Troczka et al., 2017) and Pfam annotations (<http://pfam.xfam.org/>).

## 2.2. PCR validation of *IP<sub>3</sub>R* receptors

Total RNA from *M. persicae* and *B. terrestris* were extracted using Trizol reagent (Life technologies, CA, USA) or ISOLATE II RNA mini kit (Bioline, UK) following the manufacturer's guide. 4 µg of total RNA was used to synthesise cDNA in 20 µl reactions containing SuperScript® III Reverse Transcriptase (Thermo Fisher Scientific, USA) and Oligo dT (15) primers (Promega, USA), following the manufacturer's instructions. PCR primers were designed based on the in silico predicted



**Coleoptera****Hemiptera****Fig. 1.** (continued)

sequences using Geneious software v. 8.1.3 (Biomatters, Ltd., New Zealand). PCR reactions were performed in 25 µl volumes using 2 × Dreamtaq mastermix (ThermoFisher Scientific, USA) with 10 pmols of each primer and 1 µl of cDNA. Details of the PCR primers used can be found in Supplementary Tables 2 and 3. All PCR reactions were analysed on 1% (w/v) TAE agarose gels and visualised using ethidium bromide staining and UV light. PCR products were purified from the agarose gel using QIAquick gel extraction kit (Qiagen, Germany), following the manufacturer's recommended protocol, and directly sequenced using Eurofins Genomics Value Read service.

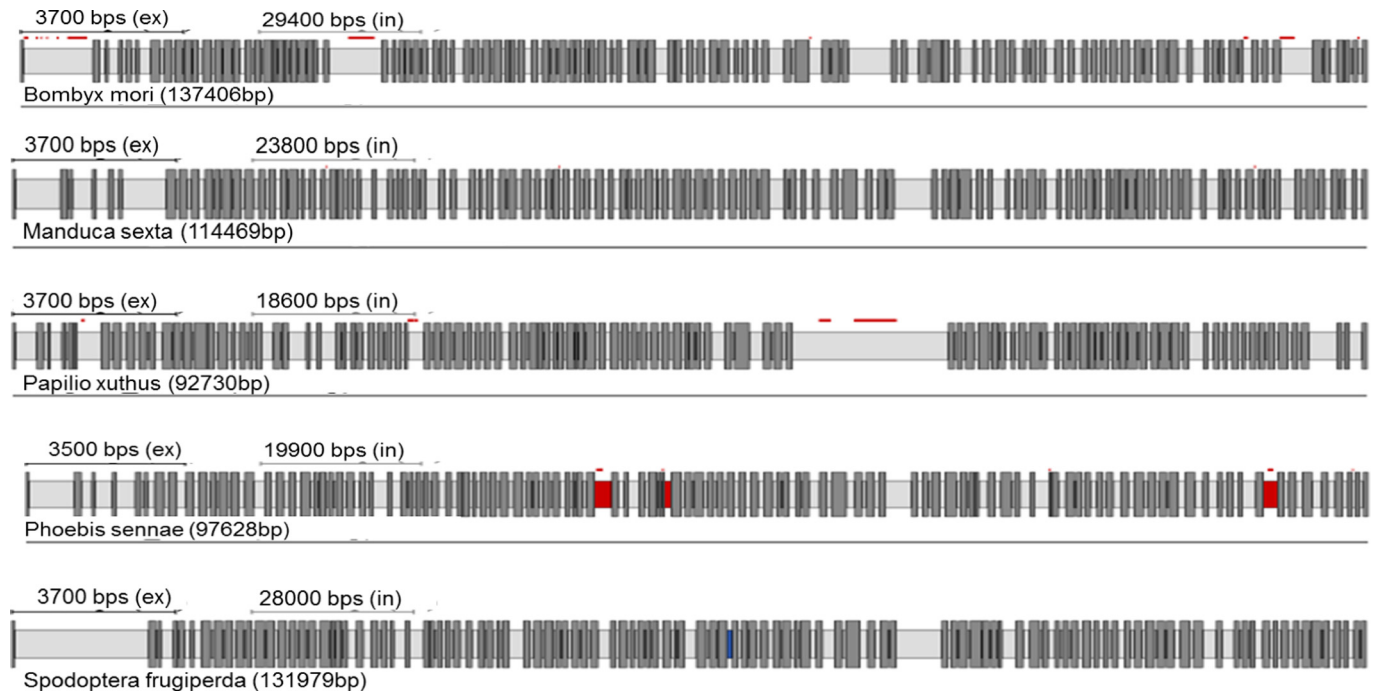
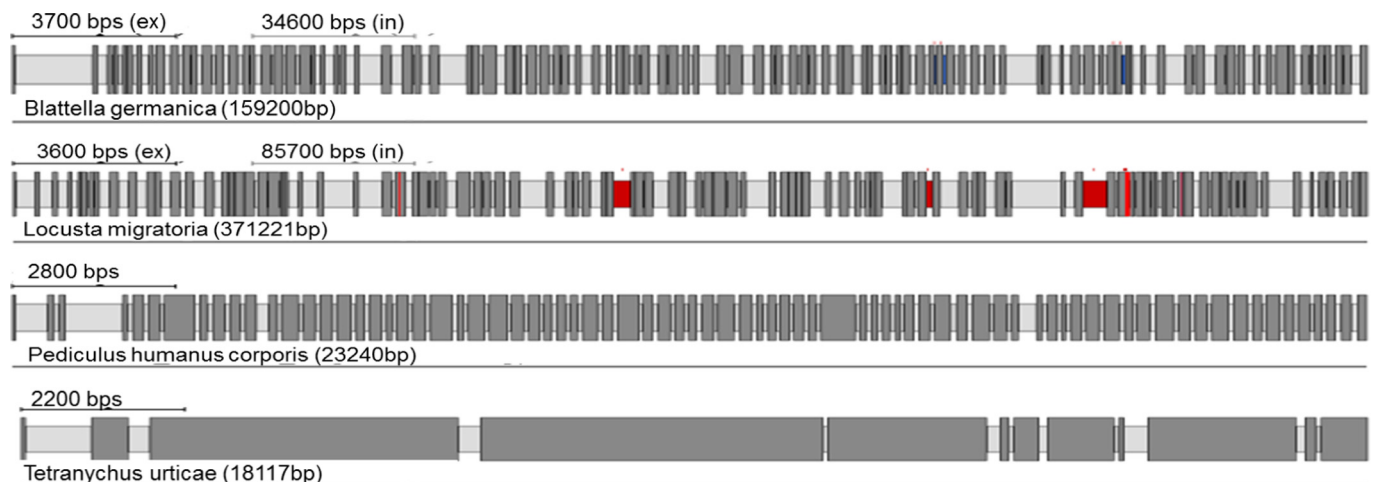
**3. Results & discussion****3.1. Structural organisation of insect RyR's**

RyR cDNA sequences and their corresponding genomic organisation have been previously confirmed experimentally in *D. melanogaster*, *M. persicae*, *T. castaneum* and *B. mori* (Takeshima et al., 1994; Liu et al., 2014; Troczka et al., 2015a; Xu et al., 2000; Kato et al., 2009). Here we have manually annotated the RyRs of a further 23 insect species. A summary of the predicted channels and intron/exon arrangements of all

26 insect species can be found in Table 1 and Fig. 1. Additional information can be found in Supplementary excel file (SUP Table 1).

Protein alignments and Pfam database searches were performed to compare RyRs from different insect species. As expected, all the insect RyRs presented the classical cytosolic motifs and domains previously annotated in *P. xylostella* (Troczka et al., 2017) including one MIR (220–400), two SPRY domains, (726–862 and 1702–1841), four RYR domains (917–1007, 1031–1120, 3075–3166 and 3220–3303), three RIH domains (503–702, 2433–2682, 4307–4423) and EF calcium binding motifs (4531–4576). The numbering is based on a consensus sequence of a MAFFT alignment of all 27 RyR sequences with the annotated *P. xylostella* RyR (Fig. 2). The transmembrane (TM) region of the channel, which according to three-dimensional reconstructions using Cryo EM structures consist of six α-helices (Yan et al., 2015; Zalk et al., 2015), was the most highly conserved region of the protein across all examined insect species.

The TM region of RyR is thought to be the binding site of diamide insecticides (Kato et al., 2009). In support of that hypothesis a glycine to glutamic acid substitution at position 4946 of the transmembrane domain of *Plutella xylostella* RyR has been shown to be a major cause of diamide resistance in this pest insect (Troczka et al., 2015b; Troczka

**Lepidoptera****Other****Fig. 1.** (continued)

et al., 2012; Steinbach et al., 2015). Recently, a novel glycine to valine substitution at this position has been identified in diamide resistant populations of *Tuta absoluta* (Roditakis et al., 2017). Additionally, three other mutations (E1338D, Q4594L and I4790M) have been associated with diamide resistant strains of *P. xylostella* (Guo et al., 2014). The equivalent of I4790M, located in the second TM helix and coming to close proximity to G4946 in a 3D model of insect RyR, was also found in some resistant populations of *T. absoluta* (Roditakis et al., 2017). Interestingly, the glycine residue at position 4946 appears to be conserved in most insect species, apart from *B. antarctica* and *T. urticae* which have an alanine in this position and *F. virgata* which has an arginine. It remains to be tested, however, whether these changes have any implications on diamide binding. Additionally, the neighboring amino acids in these later three species have a lower level of conservation in comparison to other insects (SUP Fig. 1). This amino acid residue “flexibility” within a highly conserved region could be one of

the reasons diamide resistance mutations have emerged relatively quickly and without any apparent fitness costs (Ribeiro et al., 2014). In contrast to G4946 the isoleucine at position 4790 appears to be unique to lepidopterans, with all other insect species analysed in this study having a methionine or valine (found only in *F. virgata*). Therefore, it is hypothesised that an isoleucine at position 4790 may confer selectivity for some diamides towards lepidopteran insects. Q4594 is located in divergent region one with several different amino acids being found at this position, the most common being lysine (present in Coleoptera, Hymenoptera and some Diptera), glutamine (Lepidoptera), histidine (some Hemiptera), arginine (*A. gambiae*) and asparagine (*M. persicae*). E1338 is located between the first SPRY domain and divergent region two and like Q4594 shows little amino acid conservation with various amino acids (valine, glycine, serine, glutamine, aspartic acid, glutamine) found in different species.



**Fig. 2.** MAFFT alignment and Pfam domain mapping of annotated RyR sequences vs *P. xylostella* RyR. Red arrows indicate individual transmembrane helices. (For interpretation of the references to colour in this figure legend, the reader is referred to the web version of this article.)

*In silico* annotation of *M. persicae* IP<sub>3</sub>R predicted a relatively larger channel compared to other insects. With a predicted ORF of 11,373 bp, *M. persicae* IP<sub>3</sub>R was projected to encode a 3790 aa protein, making it approximately 1000 aa larger than any other insect IP<sub>3</sub>R reported in this study, including those insects in the order hemiptera (e.g. *Bemisia tabaci* (Guo et al., 2017)). Protein alignment of the *M. persicae* channel with *D. melanogaster* IP<sub>3</sub>R indicated that the additional amino acids are scattered across the entire length of the protein (Fig. 5). Some of these insertions are present in functionally important domains, which could have a significant impact on the channels function. Interestingly the majority of insertions appear to be within the middle of the exons as opposed to 5' or 3' ends. Protein blast analysis of this predicted protein provided a good match up (over 90% identity) with other computationally predicted aphid IP<sub>3</sub>Rs, from pea aphid (*Acyrtosiphon pisum*, NCBI Acc. XP\_001947344.2, encoding a 3831aa protein) and two predicted Russian wheat aphid alternatively spliced forms (*Diuraphis noxia*, NCBI Acc. XP\_015373414.1 and XP\_015373416.1, encoding proteins of 3816 and 3788 aa respectively). RT-PCR validation of the *in-silico* prediction for *M. persicae* IP<sub>3</sub>R confirmed that the receptor is much larger in this species in comparison to other insects, and that the predicted extra amino acids are present in the cDNA and are not intronic sequences. These larger IP<sub>3</sub>R channels appear to be unique to aphids. Pfam analysis of the protein sequence matches it with IP<sub>3</sub>R receptors, with conserved domains: Ins145\_P3\_rec (45–313), two MIR domains (345–476, 530–583), RIH (627–860) and the ion transport domain (3404–3624). The reason for a much larger IP<sub>3</sub>R in aphids is not apparent and we have found no evidence of similarly enhanced IP<sub>3</sub>Rs in other insect orders, so there is no clear evolutionary lineage. IP<sub>3</sub>R is the more ancient of the two channels studied (Alzayady et al., 2015). Evidence for larger IP<sub>3</sub>Rs-like channels (over 3000 amino acids) was reported in protozoan species such as *Paramecium* (Ladenburger and Plattner, 2011) and the filasterean *Capsaspora owczarzakii* (Alzayady et al., 2015); however these channels show very little conservation to the aphid protein. A significantly increased receptor size clearly has the potential to have a substantial impact on the channel's physiology and regulation. It has also been previously reported that aphids have an unusual heterodimeric voltage-gated cation channel, with close sequence homology with the voltage-gated sodium channel in other insects, albeit with an altered selectivity filter and being encoded by two unique heteromers (Amey et al., 2015; Zuo et al., 2016; Jiang et al., 2017). It is worth speculating that significant structural changes to at least two important ion channels could be indicative of a unique ion



**Table 2**  
Summary of annotated sequences for inositol 1,4,5-triphosphate receptors.

Order	Species	Exon	Accession no.	Protein (AA)	Gene (bp)	Genome (Mb)
Diptera	<i>Anopheles gambiae</i> (African malaria mosquito)	16	XP_557157	2830	14,149	265.027
	<i>Ceratitis capitata</i> (Mediterranean fruit fly)	22	XP_012156517	2886	18,431	479.048
	<i>Drosophila melanogaster</i> (fruit fly)	19	P29993	2838	10,830	143.726
	<i>Musca domestica</i> (house fly)	22		2800	32,699	750.404
	<i>Belgica antarctica</i> (Antartic midge)	8		2694	8468	89.5837
Hymenoptera	<i>Apis mellifera</i> (honey bee)	43		2727	27,950	250.287
	<i>Bombus terrestris</i> (buff-tailed bumblebee)	43	XP_003394052	2727	34,077	248.654
	<i>Nasonia vitripennis</i> (jewel wasp)	38	XP_016839078	2745	26,320	295.781
	<i>Megachile rotundata</i> (alfalfa leafcutting bee)	42		2724	39,393	272.661
	<i>Harpegnathos saltator</i> (Jerdon's jumping ant)	44	XP_011151642	2741	37,606	294.466
Coleoptera	<i>Tribolium castaneum</i> (red flour beetle)	27	NP_001308600	2724	11,552	165.944
	<i>Dendroctonus ponderosae</i> (mountain pine beetle)	27		2700	15,589	252.848
	<i>Anoplophora glabripennis</i> (Asian longhorned beetle)	26		2706	12,268	707.712
	<i>Hypothenemus hampei</i> (coffee berry borer)	26		2692	10,408	151.272
	<i>Myzus persicae</i> (green peach aphid)	49		3790	24,399	347.313
Hemiptera	<i>Cimex lectularius</i> (bed bug)	49	XP_014243514	2735	26,666	650.478
	<i>Rhodnius prolixus</i> (assassin bug)	43		2634	40,691	706.824
	<i>Ferrisia virgata</i> (striped mealybug)	45		2645	25,926	304.571
	<i>Bombyx mori</i> (domestic silkworm)	58		2713	74,323	481.819
	<i>Papilio xuthus</i> (Asian swallowtail butterfly)	58		2722	32,751	243.89
Lepidoptera	<i>Manduca sexta</i> (tobacco hornworm)	58		2717	51,935	419.424
	<i>Spodoptera frugiperda</i> (fall armyworm)	58		2707	58,102	358.048
	<i>Tetranychus urticae</i> (two-spotted spider mite)	6	XP_015786315	2754	9348	90.8286
	<i>Blattella germanica</i> (German cockroach)	46		2661	219,647	2037.2
	<i>Pediculus humanus corporis</i> (human body louse)	2	XP_002425693	2680	8124	110.781
Other orders	<i>Locusta migratoria</i> (migratory locust)	46		2680	277,815	5759.8

physiology in aphids in comparison to other insects.

Initial computational prediction of *B. terrestris* IP<sub>3</sub>R projected an ORF of 8370 bp (NCBI Acc. XP\_012175773.1). However, RT-PCR validation followed by cDNA sequencing gave an ORF of 8184 bp (encoding a 2727 aa protein), which is a perfect match to another automatically predicted isoform of *B. terrestris* IP<sub>3</sub>Rs (NCBI Acc. XP\_003394052). In comparison to the initial *in silico* prediction, the PCR validated sequence is missing two predicted exons (exons 23 and 28). We therefore assume that these missing exons are not part of the canonical channel, as we did not detect them in our sequenced PCR fragments. They might, however, represent rare transcripts specific to *B. terrestris* and other Hymenopterans, as BLAST results for both exons generate hits exclusively to species in this order.

The overall protein sequence similarity between different insect orders for the RyRs and IP<sub>3</sub>Rs was 80% and 70% respectively; the Hymenoptera was the least diverse order with over 90% identity among analysed species for both channels (93.5% for RyR and 92.29% for IP<sub>3</sub>Rs).

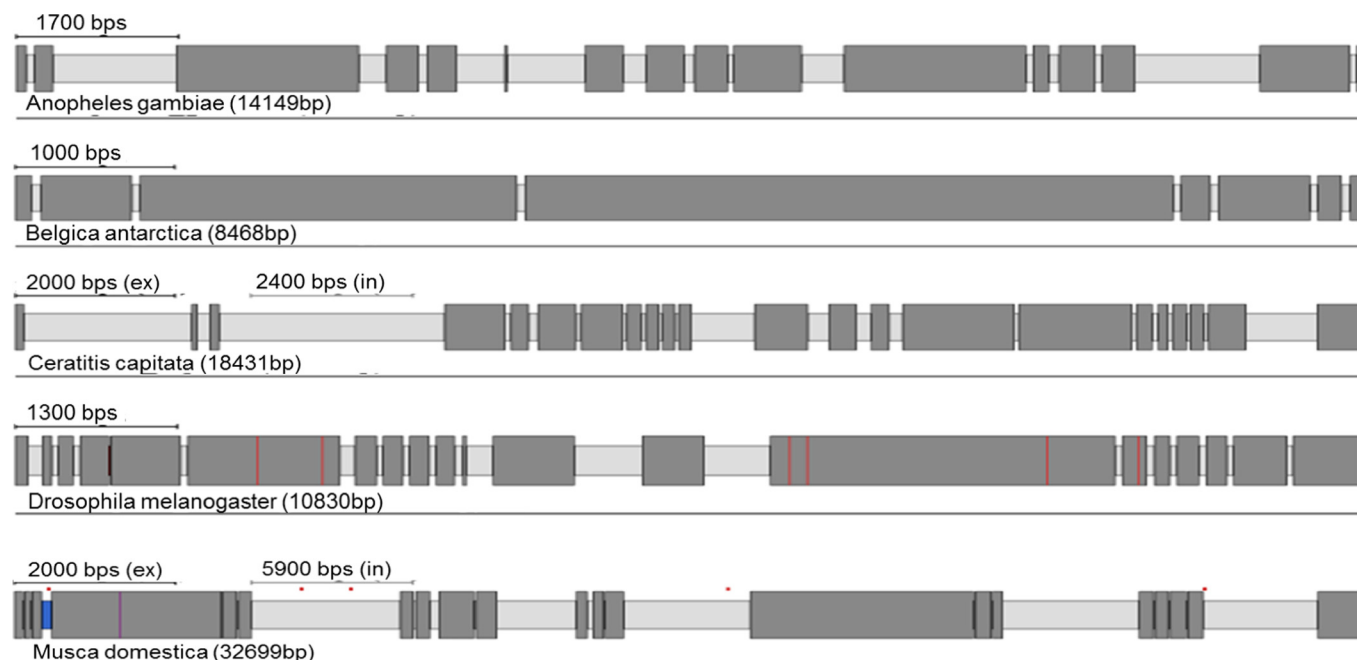
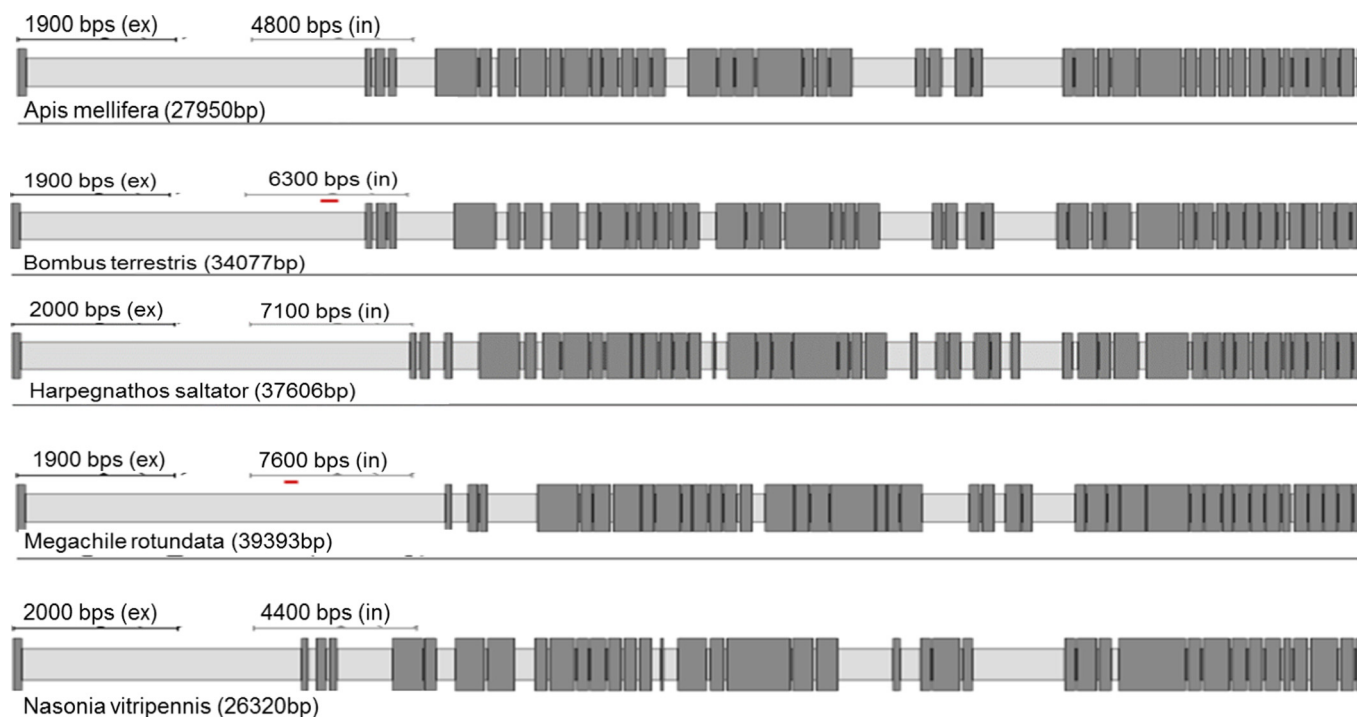
### 3.3. History of intron gain and loss within and across insect orders

There is a considerable variation in the number of introns present in RyR and IP<sub>3</sub>R genes across insect orders and other arthropods, reflected in the number of exons recorded for each species (Tables 1 & 2). However, there is generally only a small variation in the number of introns within each order, irrespectively of the genome size. For example, in Diptera, *Musca domestica* RyR has only two additional introns in comparison to *B. antarctica* despite its genome being 8.4 times larger (750 Mb and 89 Mb respectively). Substantial variation in intron number within a single order was only observed for Dipteran IP<sub>3</sub>R genes, with the flightless midge, *B. antarctica*, having only 7 introns compared with 21 introns for *M. domestica* and *C. capitata*. Species with the most complex IP<sub>3</sub>R belong to Lepidopterans (58 exons), followed by Hemipterans and Hymenopterans (over 40 exons) making them almost as complex as human IP<sub>3</sub>R genes with 63 exons for human type 1 and 2 isoforms (NCBI gene ID: 3708 and 3709). The RyRs of the representative species of the orders Diptera, Hymenoptera and Coleoptera showed significant changes in intron number in comparison to

mammalian orthologues. For Lepidoptera, Hemiptera and Orthopteroidea the total intron numbers recorded are close to the human isoforms (~105 introns) (Phillips et al., 1996).

A summary of loss and gain of introns across species is presented in the Genepainter phylogenetic 'intron distribution' trees for RyR and IP<sub>3</sub>Rs (Figs. 6 and 7). Notably within the Paraneoptera, the entire IP<sub>3</sub>R gene of *P. humanus corporis* is made up of only 2 large exons. This dramatic reduction in intron number could be related to the ectoparasitic lifestyle of the species and small genome size (Sundberg and Pulkkinen, 2015). Within the Endopterygota, a significant intron loss has occurred within RyR genes in 3 of the 4 main orders (Diptera, Coleoptera, Hymenoptera, Lepidoptera), with almost 75% of ancestral introns being lost in some Dipteran species (e.g. *D. melanogaster* with 25 introns). Only Lepidoptera (Obtectomera) have maintained a relatively high ancestral intron number whilst simultaneously showing evidence of intron gain, making their RyR genes the most complex in all of the targeted insect species included in this study. They contain up to 110 exons on average, comparable in complexity to their mammalian counterparts (Phillips et al., 1996). The same pattern is observed for the IP<sub>3</sub>Rs genes, with the most complex architecture being found in Lepidoptera (58 exons), whilst the Diptera display the greatest overall reduction in intron number (25 introns) of all the insect orders studied (with the notable exception of *P. humanus corporis* as discussed above).

Despite an overall high level of conservation at the protein (amino acid) level for both RyR and IP<sub>3</sub>R channels in insects, an extensive re-modelling of the genomic structure has resulted in a low conservation of common introns across insect orders. GenePainter analysis showed only 8 common introns conserved within RyR across the insect species looked at in this study. This number falls to only 3 when *T. urticae* (Acari) is included in the analysis. Interestingly, 4 of the common (conserved) introns are located within the first 10 introns, with a further 2 encompassing a highly-conserved exon (exon 20 in *D. melanogaster*, 39 in *A. mellifera*, and *B. mori*, 71 in *M. persicae*). Looking at the overall distribution of intron positions, it appears that the greatest number of intron losses occur towards the 3' end of the ORF (see SUP Table 1), possibly indicating the involvement of reverse transcriptase in this evolutionary process (Cohen et al., 2012). The conservation of intron-exon organisation does not appear to be linked with any particular

**Diptera****Hymenoptera**

**Fig. 3.** IP<sub>3</sub>R gene structures generated by Webscipio. Dark grey regions correspond to exons. Red dashes indicate sequence gaps, blue indicate some uncertainty in intron assignment (non-canonical intron boundaries). (For interpretation of the references to colour in this figure legend, the reader is referred to the web version of this article.)

structural features. All of the conserved intron-exon junctions occur within the cytosolic portion of the protein. The highest level of conservation is found in the introns surrounding a mutually exclusive splice site in the second SPRY domain, with *M. persicae* being the outlier. The second highest conserved pair of introns is found around the predicted calmodulin/Apo-calmodulin interaction site, which also appears to be

alternatively spliced in some species. In contrast, there are 34 unique introns detected across all species (Fig. 8). There are no conserved introns for IP<sub>3</sub>Rs and only 2 conserved introns if *T. urticae* and *P. humanus corporis* are excluded. However, there are 56 unique introns found across the 26-species studied (Fig. 9). In comparison to the RyRs, the IP<sub>3</sub>R gene structure is less well conserved with a much higher



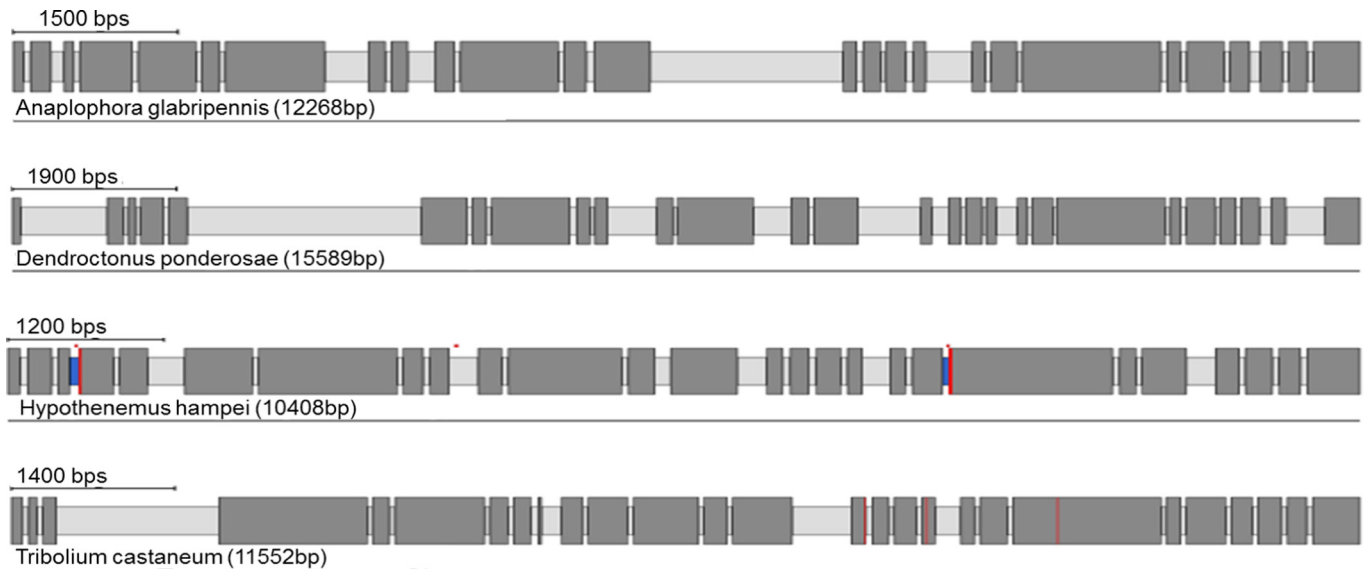
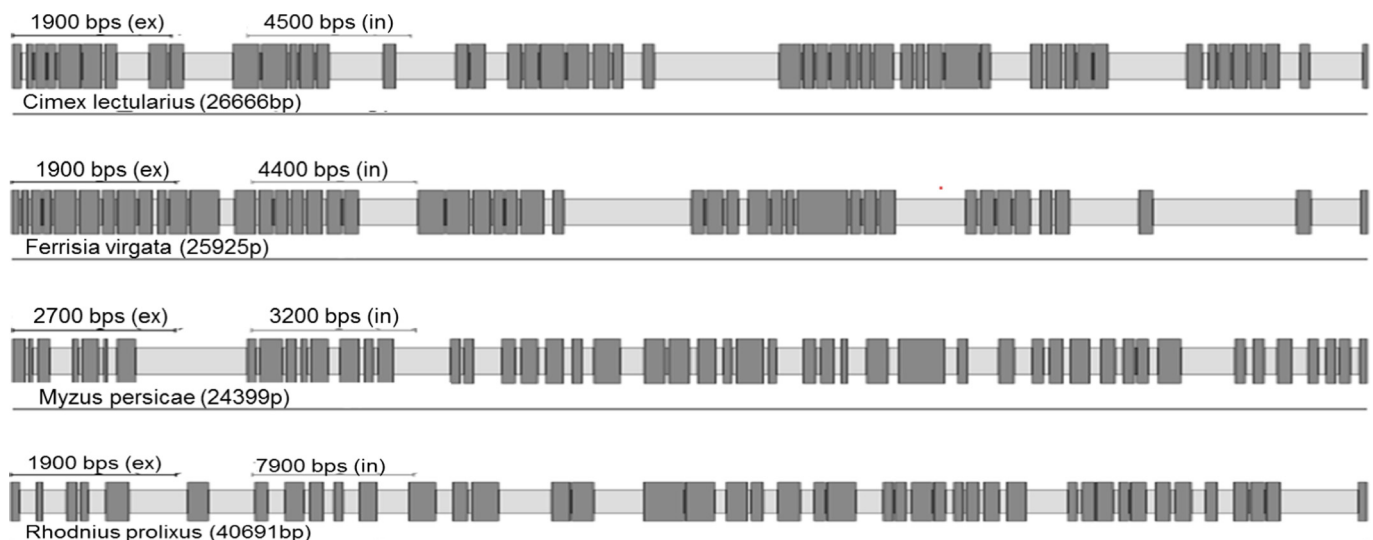
**Coleoptera****Hemiptera**

Fig. 3. (continued)

proportion of unique introns in relation to the total intron number.

### 3.4. Alternative splicing of RyR and $IP_3R$

Fully annotated gene structures can elucidate further useful information such as the regulatory mechanisms governing gene expression and the probability of alternative splicing (Chorev and Carmel, 2012). Understanding splicing regulation is a difficult challenge as the spliceosome is one of the most complicated molecular complexes, consisting of over 150 proteins (Wahl et al., 2009). Point mutations in the genomic structure may lead to modulation of the splicing machinery resulting in exon skipping (Cartegni et al., 2002). Such an event in the nicotinic acetylcholine receptor has already been linked with resistance to the insecticide spinosad in *Tuta absoluta* (Berger et al., 2016). Intron size and number have also been shown to directly correspond to splicing diversity (Chorev and Carmel, 2012; Fox-Walsh et al., 2005).

RyRs are known to possess an inherently complex genomic organisation and several alternative spliced isoforms have been reported in

insects (Xu et al., 2000; X. Wang et al., 2012; Puente et al., 2000). A common (mutually exclusive) alternative splice site has been found in 21 of the 26 studied species, the exceptions being *P. humanus*, *T. urticae*, *B. antarctica*, *C. lectularius* and the previously reported *M. persicae* (Troczka et al., 2015a). This site is located within the second SPRY domain in the N-terminal part of the channel (Fig. 10). SPRY domains are found in many mammalian proteins and are thought to be linked with immune responses (D'Cruz et al., 2013). In mammalian RyR1, the second SPRY domain is a site of interaction with the II-III loops of  $Ca_v1.1$  and also with scorpion toxin A (Tae et al., 2009). Although insect RyRs are thought not to be directly linked with  $Ca_v1.1$  channels (Takekura and Franzini-Armstrong, 2002), alternative exons in this region might play important roles in modulating the interaction of insect RyRs with other regulatory proteins. To date alternative exons have been best described in Lepidopteran species (Wang et al., 2013; J. Wang et al., 2012; Sun et al., 2015; Wu et al., 2013; Cui et al., 2013). As highlighted in Fig. 8, exon version A is present in all species lacking an alternative exon. Thus, version A is likely to be the most common splice form. In *M. persicae* this exon is fused with a neighboring exon

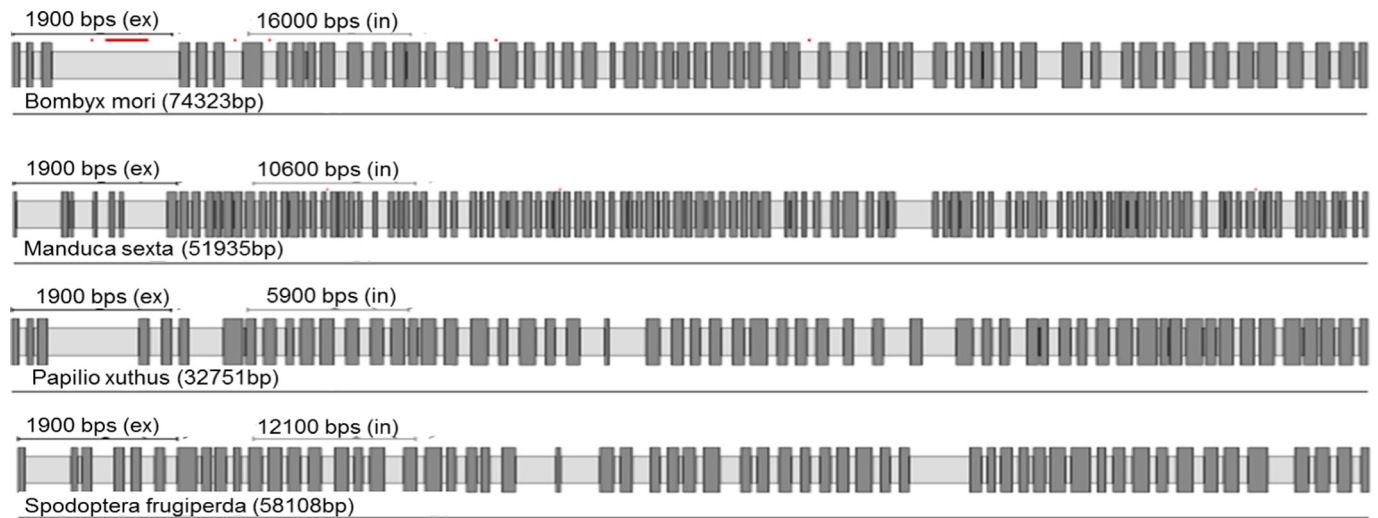
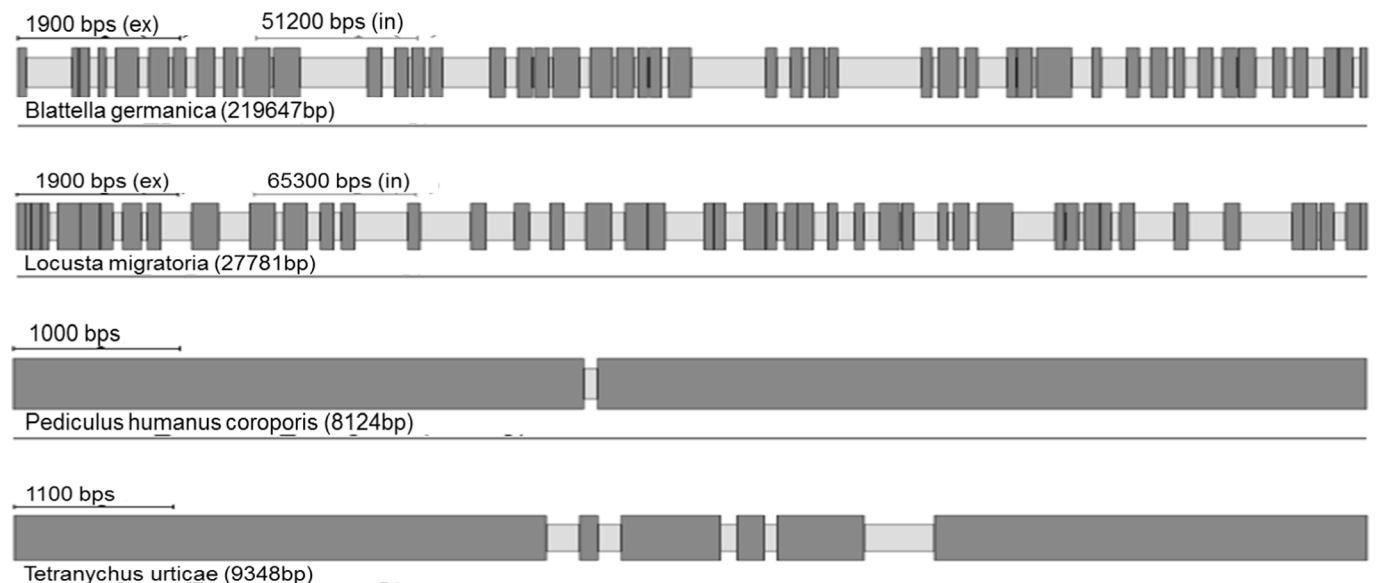
**Lepidoptera****Other**

Fig. 3. (continued)

indicating a clear intron loss event (Troczka et al., 2015a).

Apart from mutually exclusive exons, there is growing evidence, especially in Lepidoptera, of a number of deletions and insertions which result in a greater diversity of detectable splice forms in comparison to other insect species, as shown by the extensive splice forms detected in *P. xylostella* (X. Wang et al., 2012).

We did not attempt to map mutually exclusive exons in insect IP<sub>3</sub>Rs due to the scarcity of experimentally obtained mRNA sequences. However, due to this paucity of validated cDNA's the existence of such exons cannot be dismissed. Alternative splicing of IP<sub>3</sub>Rs is well documented in mammals (Foskett et al., 2007) and at least one of these splice sites appears to be conserved in *D. melanogaster* (Sorrentino et al., 2000).

**4. Conclusions**

Despite an ever-growing number of insect genomes becoming publicly available the quality of many of them remains problematic. Short contig lengths and a high degree of fragmentation make it challenging

to fully annotate large genes such as RyRs and IP<sub>3</sub>Rs (Mackrill, 2012). Additionally, automatic annotations can omit certain sections of the gene (usually the 1st exon) if it is positioned a long distance from the rest of the gene and no reference transcriptome data is available. Manual curation of important genes and gene families is required to verify and improve genomic data. In the case of insects, validation of automatically annotated genes has not been done for many species. Certain insect orders remain over represented in the wet biology due to their importance to agriculture or disease control. Our study shows that despite a relatively high protein homology, the gene architecture of proteins can differ substantially among different insect orders. We have shown that there is a substantial variation in exon number and overall gene size for both RyR and IP<sub>3</sub>R channels and very little intron conservation across different species. Structural variation of genes coding for highly conserved proteins is likely to contribute to a great diversity in potential mRNAs among insects allowing for the existence of species and order-specific splice variants.

Supplementary data to this article can be found online at <https://doi.org/10.1016/j.gene.2018.05.075>.

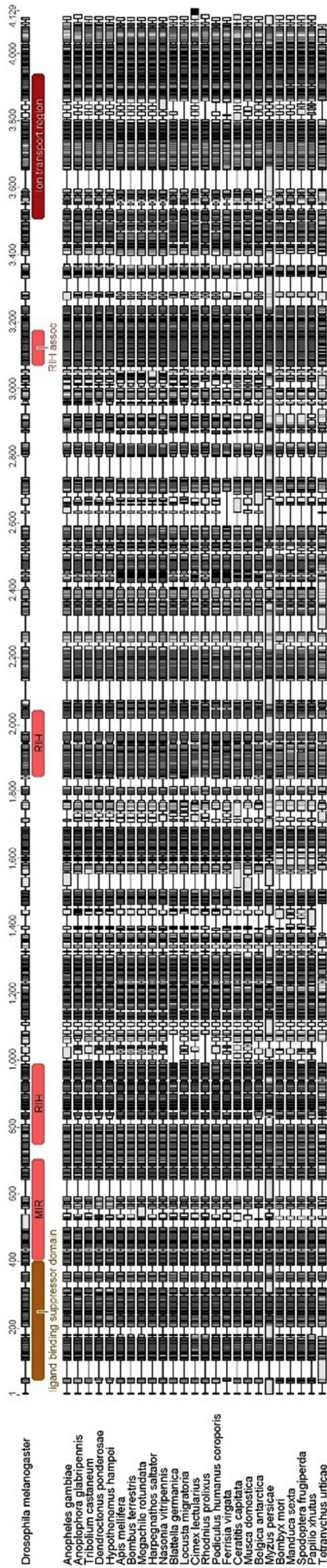


Fig. 4. MAFFT alignment and Pfam domain map of annotated insect IP<sub>3</sub>R sequences.

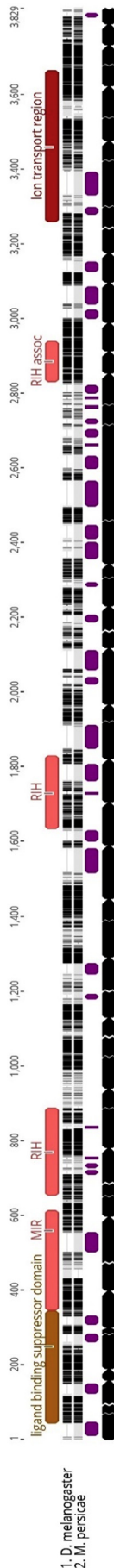
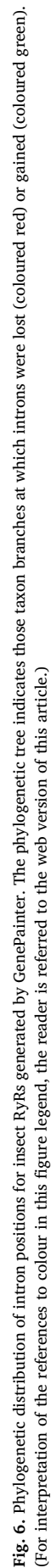
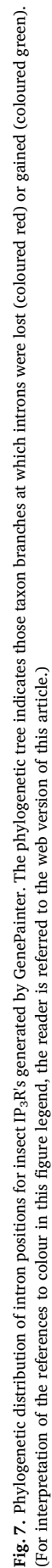
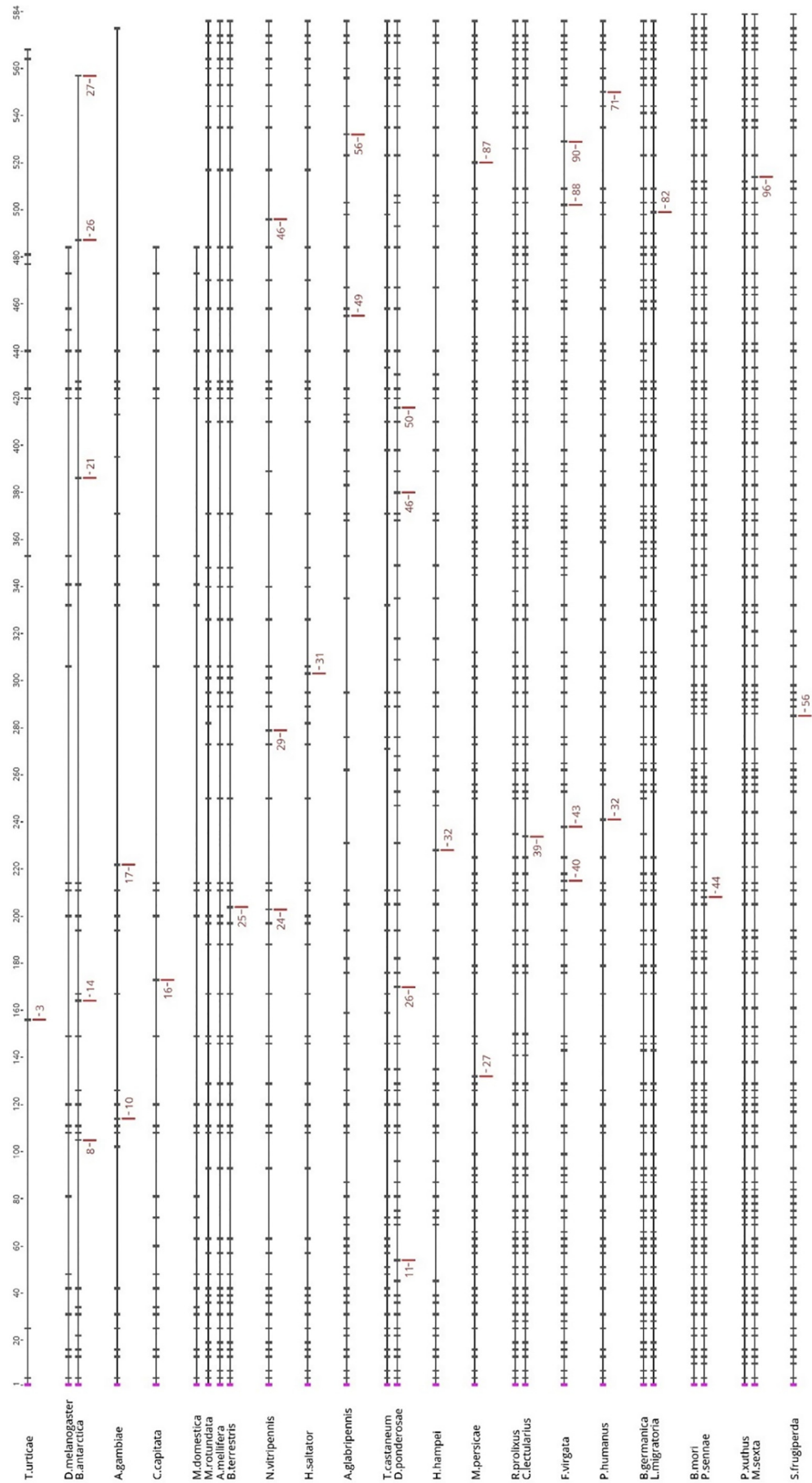


Fig. 5. Alignment of *D. melanogaster* IP<sub>3</sub>R with *M. persicae* IP<sub>3</sub>R. Black arrows indicate individual exons. The approximate location of additional amino acids found in the aphid channel are indicated in purple. There are 36 individual insertions in the aphid channel with the largest being 63 amino acids in length. IP<sub>3</sub>R functional domains are mapped on the *D. melanogaster* sequence. (For interpretation of the references to colour in this figure legend, the reader is referred to the web version of this article.)









**Fig. 8.** Gene structure alignment for insect RyRs obtained from Genepainter. Each dash corresponds to an intron overlaid on a protein alignment. To improve clarity the size of each exon is not representative of the actual exon size. Red dashes indicate unique introns and their number in individual species. (For interpretation of the references to colour in this figure legend, the reader is referred to the web version of this article.)

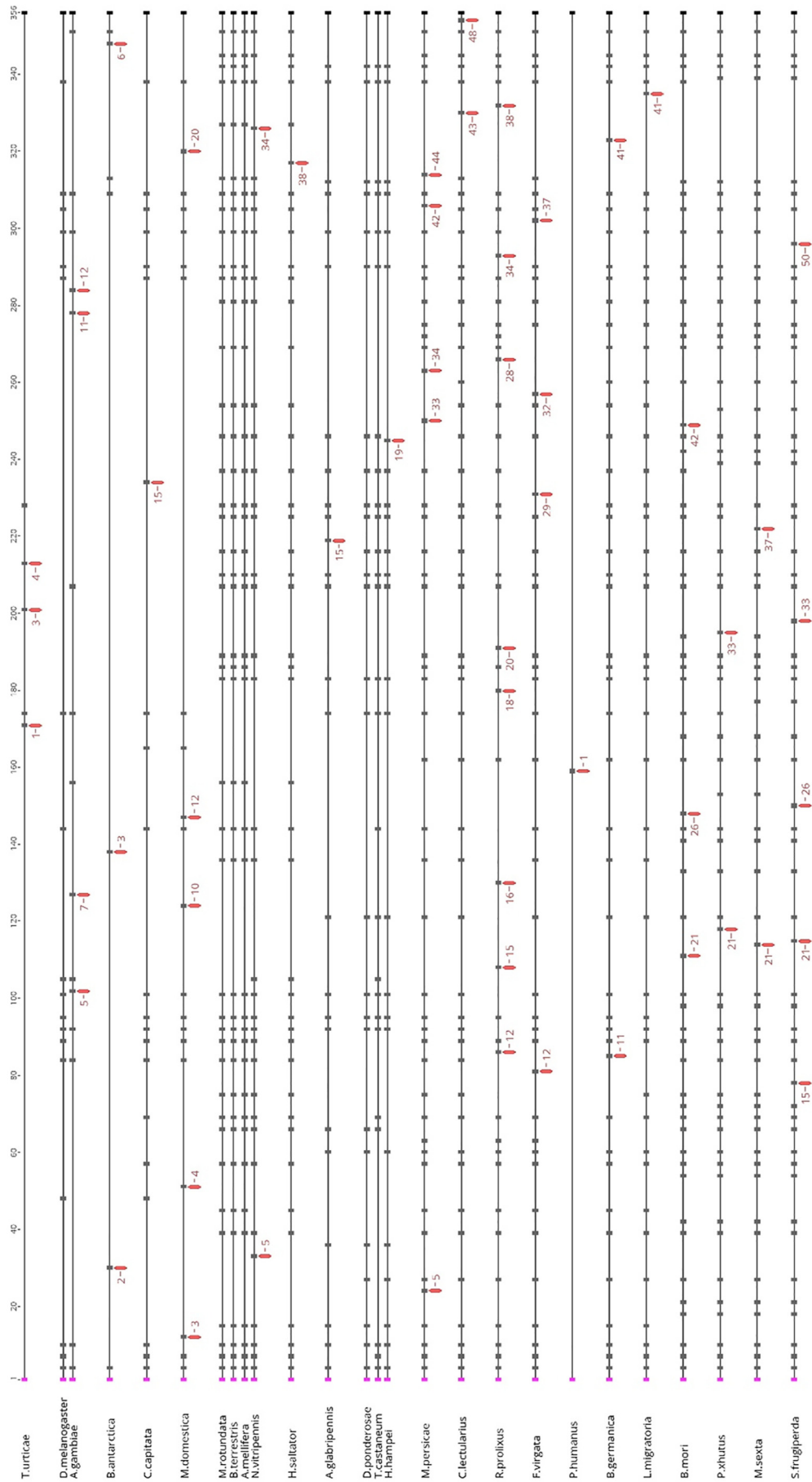


**Fig. 9.** Gene structure alignment for IP<sub>3</sub>Rs obtained from Genepainter. Each dash corresponds to an intron. To improve clarity the size of each exon is not representative of the actual exon size. Red dashes indicate unique introns and their number in individual species. In total there are 56 unique introns mapped on the alignment. (For interpretation of the references to colour in this figure legend, the reader is referred to the web version of this article.)

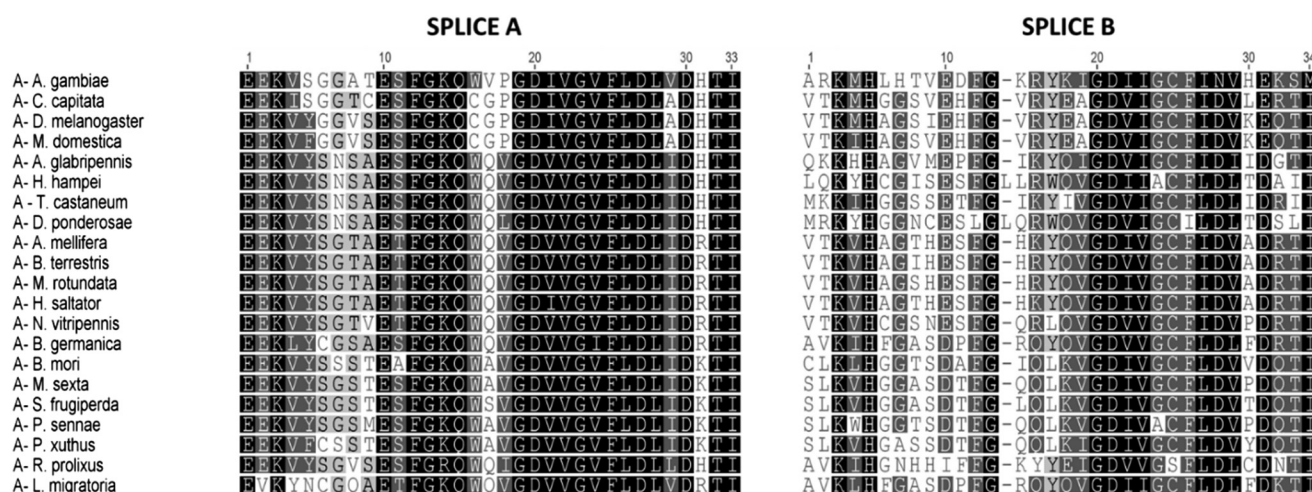


Fig. 10. Multiple alignment of a mutually exclusive splice site found in 21 of the analysed insect RyR sequences.

## Conflicts of interest

The authors declare no conflict of interest. The funding sponsors had no role in the design of the study; in the collection, analyses, or interpretation of data; in the writing of the manuscript, and in the decision to publish the results.

## Acknowledgments

Dr. T.G. Emyr Davies and Dr. Rafael A. Homem receive grant-aided support from the Biotechnology and Biological Sciences Research Council's Industrial Strategy Challenge Fund (BBS/OS/CP/000001). Ewan Richardson is in receipt of an Industrial studentship jointly funded by the BBSRC and Bayer CropScience (BB/N504075/1).

## Appendix A. List of genome projects and Accessions used for data generation with associated peer reviewed publications (where appropriate)

*Tetranychus urticae* (BioProjects: PRJNA315122, PRJEA71041) (Grbic et al., 2011), *Drosophila melanogaster* (chromosome 2R ref. seq: NT\_033778.4) (Hoskins et al., 2007), *Anopheles gambiae* (chromosome 3L ref. seq: NT\_078267.5) (Holt et al., 2002), *Ceratitidis capitata* (BioProjects: PRJNA201381, PRJNA168120) (Papanicolaou et al., 2016), *Belgica antarctica* (BioProject: PRJNA172148) (Kelley et al., 2014), *Musca domestica* (BioProject: PRJNA210139) (Scott et al., 2014), *Megachile rotundata* (BioProjects: PRJNA87021, PRJNA66515), *Apis mellifera* (Linkage group: NC\_007071.3, BioProject: PRJNA10625) (Honeybee Genome Sequencing Consortium, 2006), *Bombus terrestris* (BioProjects: PRJNA68545, PRJNA45869) (Sadd et al., 2015), *Nasonia vitripennis* (BioProjects: PRJNA20073, PRJNA13660) (Werren et al., 2010), *Harpegnathos saltator* (BioProjects: PRJNA273397, PRJNA50203) (Bonasio et al., 2010), *Tribolium castaneum* (BioProjects: PRJNA15718, PRJNA12540) (Tribolium Genome Sequencing Consortium, 2008), *Dendroctonus ponderosae* (BioProject: PRJNA162621) (Keeling et al., 2013), *Anoplophora glabripennis* (BioProjects: PRJNA348318, PRJNA167479), *Hypothenemus hampei* (BioProject: PRJNA279497) (Vega et al., 2015), *Myzus persicae* (BioProjects: PRJNA397782, PRJNA319804), *Cimex lectularius* (BioProject: PRJNA167477) (Rosenfeld et al., 2016), *Rhodnius prolixus* (BioProject: PRJNA13648) (Mesquita et al., 2015), *Ferrisia virgata* (BioProject: PRJEB12067), *Blattella germanica* (BioProject: PRJNA203136), *Locusta migratoria* (BioProject: PRJNA185471) (Wang et al., 2014), *Pediculus humanus corporis* (BioProjects: PRJNA19807, PRJNA16223) (Kirkness et al., 2010), *Bombyx mori* (BioProject: PRJDA20217) (International

Silkworm Genome Consortium, 2008), *Papilio xuthus* (BioProject: PRJDB2956), *Manduca sexta* (BioProject: PRJNA81037) (Kanost et al., 2016), *Spodoptera frugiperda* (BioProject: PRJNA257248) (Kakumani et al., 2014), *Phoebis sennae* (BioProject: PRJNA308118) (Cong et al., 2016).

## Appendix B. Ryanodine receptor sequences (and associated NCBI Accession numbers) used for the validation alignments

*Aphis citricidus* (AKM95171.1), *Atta colombica* (KYM79740.1), *Bemisia tabaci* (AFK84957.1), *Cnaphalocrocis medinalis* (AFI80904.1), *Cerapachys biroi* (EZA52107.1), *Carpodina sasakii* (AHN16453.1), *Chilo suppressalis* (AFN70719.1), *Daphnia pulex* (EFX89429.1), *Dialeurodes citri* (AKM95170.1), *Helicoverpa armigera* (AHB33498.1), *Homo sapiens* RyR1 (AAC51191.1), *Homo sapiens* RyR2 (CAA66975.1), *Homo sapiens* RyR3 (CAA04798.1), *Laodelphax striatella* (AFK84959.1), *Leptinotarsa decemlineata* (AHW99830), *Lucilia cuprina* (KNC23059.1), *Melipona quadrifasciata* (KOX73585.1), *Nilaparvata lugens* (KF306296.1), *Ostrinia furnacalis* (AGH68757.1), *Pieris rapae* (AGI62938.1), *Plutella xylostella* (AET09964.1), *Sogatella furcifera* (AIA23859), *Spodoptera exigua* (AFC36359.1), *Trachymyrmex cornetzi* (KYN11971.1), *Tuta absoluta* (APC65631.1).

## References

- Alzayady, K.J., et al., 2015. Tracing the evolutionary history of inositol, 1, 4, 5-trisphosphate receptor: insights from analyses of *Capsaspora owczarzakii* Ca<sup>2+</sup> release channel orthologs. *Mol. Biol. Evol.* 32 (9), 2236–2253.
- Amey, J.S., et al., 2015. An evolutionarily-unique heterodimeric voltage-gated cation channel found in aphids. *FEBS Lett.* 589 (5), 598–607.
- Berger, M., et al., 2016. Insecticide resistance mediated by an exon skipping event. *Mol. Ecol.* 25 (22), 5692–5704.
- Bonasio, R., et al., 2010. Genomic comparison of the ants *Camponotus floridanus* and *Harpegnathos saltator*. *Science* 329 (5995), 1068–1071.
- Cartegni, L., Chew, S.L., Krainer, A.R., 2002. Listening to silence and understanding nonsense: exonic mutations that affect splicing. *Nat. Rev. Genet.* 3 (4), 285–298.
- Chorev, M., Carmel, L., 2012. The function of introns. *Front. Genet.* 3, 55.
- Cohen, N.E., Shen, R., Carmel, L., 2012. The role of reverse transcriptase in intron gain and loss mechanisms. *Mol. Biol. Evol.* 29 (1), 179–186.
- Cong, Q., et al., 2016. Speciation in cloudless sulphurs gleaned from complete genomes. *Genome Biol. Evol.* 8 (3), 915–931.
- Cordova, D., et al., 2006. Anthranilic diamides: a new class of insecticides with a novel mode of action, ryanodine receptor activation. *Pestic. Biochem. Physiol.* 84 (3), 196–214.
- Cui, L., et al., 2013. Molecular cloning, characterization and expression profiling of a ryanodine receptor gene in Asian corn borer, *Ostrinia furnacalis* (Guenee). *PLoS One* 8 (10).
- Dale, R.P., et al., 2010. Identification of ion channel genes in the *Acyrtosiphon pisum* genome. *Insect Mol. Biol.* 19, 141–153.
- D'Cruz, A.A., et al., 2013. Structure and function of the SPRY/B30.2 domain proteins involved in innate immunity. *Protein Sci.* 22 (1), 1–10.
- Ebbinghaus-Kintscher, U., et al., 2007. Flubendiamide, the first insecticide with a novel



- mode of action on insect ryanodine receptors. *Pflanzenschutz-Nachrichten Bayer* 60 (2), 117–140.
- Fill, M., Copello, J.A., 2002. Ryanodine receptor calcium release channels. *Physiol. Rev.* 82 (4), 893–922.
- Foskett, J.K., et al., 2007. Inositol trisphosphate receptor  $\text{Ca}^{2+}$  release channels. *Physiol. Rev.* 87 (2), 593–658.
- Fox-Walsh, K.L., et al., 2005. The architecture of pre-mRNAs affects mechanisms of splice-site pairing. *Proc. Natl. Acad. Sci. U. S. A.* 102 (45), 16176–16181.
- Grbic, M., et al., 2011. The genome of *Tetranychus urticae* reveals herbivorous pest adaptations. *Nature* 479 (7374), 487–492.
- Guo, L., et al., 2014. Novel mutations and mutation combinations of ryanodine receptor in a chlorantraniliprole resistant population of *Plutella xylostella* (L.). *Sci. Rep.* 4, 6924.
- Guo, L., et al., 2017. Silence of inositol 1,4,5-trisphosphate receptor expression decreases cyantraniliprole susceptibility in *Bemisia tabaci*. *Pestic. Biochem. Physiol.* 142, 162–169.
- Hamilton, S.L., Serysheva, I.I., 2009. Ryanodine receptor structure: progress and challenges. *J. Biol. Chem.* 284 (7), 4047–4051.
- Hammesfahr, B., et al., 2013. GenePainter: a fast tool for aligning gene structures of eukaryotic protein families, visualizing the alignments and mapping gene structures onto protein structures. *BMC Bioinf.* 14, 77.
- Hatje, K., et al., 2011. Cross-species protein sequence and gene structure prediction with fine-tuned Webscipio 2.0 and Scipio. *BMC Res. Notes* 4, 265.
- Holt, R.A., et al., 2002. The genome sequence of the malaria mosquito *Anopheles gambiae*. *Science* 298 (5591), 129–149.
- Honeybee Genome Sequencing Consortium, 2006. Insights into social insects from the genome of the honeybee *Apis mellifera*. *Nature* 443 (7114), 931–949.
- Hoskins, R.A., et al., 2007. Sequence finishing and mapping of *Drosophila melanogaster* heterochromatin. *Science* 316 (5831), 1625–1628.
- International Silkworm Genome Consortium, 2008. The genome of a lepidopteran model insect, the silkworm *Bombyx mori*. *Insect Biochem. Mol. Biol.* 38 (12), 1036–1045.
- Jiang, X.Z., et al., 2017. Characterization of an insect heterodimeric voltage-gated sodium channel with unique alternative splicing mode. *Comp. Biochem. Physiol. B Biochem. Mol. Biol.* 203, 149–158.
- Kakumani, P.K., et al., 2014. A draft genome assembly of the army worm, *Spodoptera frugiperda*. *Genomics* 104 (2), 134–143.
- Kanost, M.R., et al., 2016. Multifaceted biological insights from a draft genome sequence of the tobacco hornworm moth, *Manduca sexta*. *Insect Biochem. Mol. Biol.* 76, 118–147.
- Kapustin, Y., et al., 2008. Splign: algorithms for computing spliced alignments with identification of paralogs. *Biol. Direct* 3, 20.
- Kato, K., et al., 2009. Molecular characterization of flubendiamide sensitivity in the *Lepidopterous ryanodine receptor*  $\text{Ca}^{2+}$  release channel. *Biochemistry* 48 (43), 10342–10352.
- Keeling, C.I., et al., 2013. Draft genome of the mountain pine beetle, *Dendroctonus ponderosae* Hopkins, a major forest pest. *Genome Biol.* 14 (3), R27.
- Kelley, J.L., et al., 2014. Compact genome of the Antarctic midge is likely an adaptation to an extreme environment. *Nat. Commun.* 5, 4611.
- Kirkness, E.F., et al., 2010. Genome sequences of the human body louse and its primary endosymbiont provide insights into the permanent parasitic lifestyle. *Proc. Natl. Acad. Sci. U. S. A.* 107 (27), 12168–12173.
- Ladenburger, E.M., Plattner, H., 2011. Calcium-release channels in paramyotom. *Genomic expansion, differential positioning and partial transcriptional elimination*. *PLoS One* 6 (11), e27111.
- Liu, Y.P., et al., 2014. Comparative characterization of two intracellular  $\text{Ca}^{2+}$ -release channels from the red flour beetle, *Tribolium castaneum*. *Sci. Rep.* 4.
- Ludtke, S.J., et al., 2011. Flexible architecture of IP3R1 by Cryo-EM. *Structure* 19 (8), 1192–1199.
- Mackrill, J.J., 2012. Ryanodine receptor calcium release channels: an evolutionary perspective. *Adv. Exp. Med. Biol.* 740, 159–182.
- Mesquita, R.D., et al., 2015. Genome of *Rhodnius prolixus*, an insect vector of Chagas disease, reveals unique adaptations to hematophagy and parasite infection. *Proc. Natl. Acad. Sci. U. S. A.* 112 (48), 14936–14941.
- Muhlhausen, S., Hellkamp, M., Kollmar, M., 2015. GenePainter v. 2.0 resolves the taxonomic distribution of intron positions. *Bioinformatics* 31 (8), 1302–1304.
- Nauen, R., Steinbach, D., 2016. In: Horowitz, A.R., Ishaaya, I. (Eds.), *Resistance to diamide insecticides in Lepidopteran pests*, in *Advances in Insect Control and Resistance Management*. Springer International Publishing, Cham, pp. 219–240.
- Papanicolaou, A., et al., 2016. The whole genome sequence of the Mediterranean fruit fly, *Ceratitis capitata* (Wiedemann), reveals insights into the biology and adaptive evolution of a highly invasive pest species. *Genome Biol.* 17 (1), 192.
- Phillips, M.S., et al., 1996. The structural organization of the human skeletal muscle ryanodine receptor (RYR1) gene. *Genomics* 34 (1), 24–41.
- Puente, E., et al., 2000. Identification of a polymorphic ryanodine receptor gene from *Heliothis virescens* (Lepidoptera: Noctuidae). *Insect Biochem. Mol. Biol.* 30 (4), 335–347.
- Ribeiro, L.M.S., et al., 2014. Fitness costs associated with field-evolved resistance to chlorantraniliprole in *Plutella xylostella* (Lepidoptera: Plutellidae). *Bull. Entomol. Res.* 104 (1), 88–96.
- Roditakis, E., et al., 2017. Ryanodine receptor point mutations confer diamide insecticide resistance in tomato leafminer, *Tuta absoluta* (Lepidoptera: Gelechiidae). *Insect Biochem. Mol. Biol.* 80, 11–20.
- Rosenfeld, J.A., et al., 2016. Genome assembly and geospatial phylogenomics of the bed bug *Cimex lectularius*. *Nat. Commun.* 7.
- Sadd, B.M., et al., 2015. The genomes of two key bumblebee species with primitive eusocial organization. *Genome Biol.* 16, 76.
- Scott, J.G., et al., 2014. Genome of the house fly, *Musca domestica* L., a global vector of diseases with adaptations to a septic environment. *Genome Biol.* 15 (10), 466.
- Sorrentino, V., Barone, V., Rossi, D., 2000. Intracellular  $\text{Ca}^{2+}$  release channels in evolution. *Curr. Opin. Genet. Dev.* 10 (6), 662–667.
- Srikanth, S., et al., 2004. Functional properties of the *Drosophila melanogaster* inositol 1,4,5-trisphosphate receptor mutants. *Biophys. J.* 86 (6), 3634–3646.
- Steinbach, D., et al., 2015. Geographic spread, genetics and functional characteristics of ryanodine receptor based target-site resistance to diamide insecticides in diamondback moth, *Plutella xylostella*. *Insect Biochem. Mol. Biol.* 63, 14–22.
- Sun, L.N., et al., 2015. Molecular characterization of a ryanodine receptor gene from *Spodoptera exigua* and its upregulation by chlorantraniliprole. *Pestic. Biochem. Physiol.* 123, 56–63.
- Sundberg, L.R., Pulkkinen, K., 2015. Genome size evolution in macroparasites. *Int. J. Parasitol.* 45 (5), 285–288.
- Tae, H., Casarotto, M.G., Dulhunty, A.F., 2009. Ubiquitous SPRY domains and their role in the skeletal type ryanodine receptor. *Eur. Biophys. J.* 39 (1), 51–59.
- Takekura, H., Franzini-Armstrong, C., 2002. The structure of  $\text{Ca}^{2+}$  release units in arthropod body muscle indicates an indirect mechanism for excitation-contraction coupling. *Biophys. J.* 83 (5), 2742–2753.
- Takeshima, H., et al., 1994. Isolation and characterization of a gene for a ryanodine receptor/calcium release channel in *Drosophila melanogaster*. *FEBS Lett.* 337 (1), 81–87.
- Tribolium Genome Sequencing Consortium, et al., 2008. The genome of the model beetle and pest *Tribolium castaneum*. *Nature* 452 (7190), 949–955.
- Troczka, B., et al., 2012. Resistance to diamide insecticides in diamondback moth, *Plutella xylostella* (Lepidoptera: Plutellidae) is associated with a mutation in the membrane-spanning domain of the ryanodine receptor. *Insect Biochem. Mol. Biol.* 42 (11), 873–880.
- Troczka, B.J., et al., 2015a. Molecular cloning, characterisation and mRNA expression of the ryanodine receptor from the peach-potato aphid, *Myzus persicae*. *Gene* 556 (2), 106–112.
- Troczka, B.J., et al., 2015b. Stable expression and functional characterisation of the diamondback moth ryanodine receptor G4946E variant conferring resistance to diamide insecticides. *Sci. Rep.* 5, 14680.
- Troczka, B.J., et al., 2017. Rapid selection for resistance to diamide insecticides in *Plutella xylostella* via specific amino acid polymorphisms in the ryanodine receptor. *Neurotoxicology* 60, 224–233.
- Vega, F.E., et al., 2015. Draft genome of the most devastating insect pest of coffee worldwide: the coffee berry borer, *Hypothenemus hampei*. *Sci. Rep.* 5.
- Wahl, M.C., Will, C.L., Luhrmann, R., 2009. The spliceosome: design principles of a dynamic RNP machine. *Cell* 136 (4), 701–718.
- Wang, X., et al., 2012. Molecular cloning, characterization and mRNA expression of a ryanodine receptor gene from diamondback moth, *Plutella xylostella*. *Pestic. Biochem. Physiol.* 102 (3), 204–212.
- Wang, J., et al., 2012. Molecular characterization of a ryanodine receptor gene in the rice leafhopper, *Cnaphalocrocis medinalis* (Guenée). *PLoS One* 7 (5), e36623.
- Wang, J., et al., 2013. Molecular cloning and mRNA expression of a ryanodine receptor gene in the cotton bollworm, *Helicoverpa armigera*. *Pestic. Biochem. Physiol.* 107, 327–333.
- Wang, X.H., et al., 2014. The locust genome provides insight into swarm formation and long-distance flight. *Nat. Commun.* 5, 1–9.
- Werren, J.H., et al., 2010. Functional and evolutionary insights from the genomes of three parasitoid Nasonia species. *Science* 327 (5963), 343–348.
- Wu, S., et al., 2013. Molecular and cellular analyses of a ryanodine receptor from hemocytes of *Pieris rapae*. *Dev. Comp. Immunol.* 41 (1).
- Xu, X.H., et al., 2000. Molecular cloning of cDNA encoding a *Drosophila* ryanodine receptor and functional studies of the carboxyl-terminal calcium release channel. *Biophys. J.* 78 (3), 1270–1281.
- Yan, Z., et al., 2015. Structure of the rabbit ryanodine receptor RyR1 at near-atomic resolution. *Nature* 517 (7532), 50.
- Yandell, M., Ence, D., 2012. A beginner's guide to eukaryotic genome annotation. *Nat. Rev. Genet.* 13 (5), 329–342.
- Yoshikawa, S., et al., 1992. Molecular cloning and characterization of the inositol 1,4,5-trisphosphate receptor in *Drosophila melanogaster*. *J. Biol. Chem.* 267 (23), 16613–16619.
- Zalk, R., et al., 2015. Structure of a mammalian ryanodine receptor. *Nature* 517 (7532), 44–49.
- Zuo, Y., et al., 2016. Expression patterns, mutation detection and RNA interference of *Rhopalosiphum padi* voltage-gated sodium channel genes. *Sci. Rep.* 6, 30166.